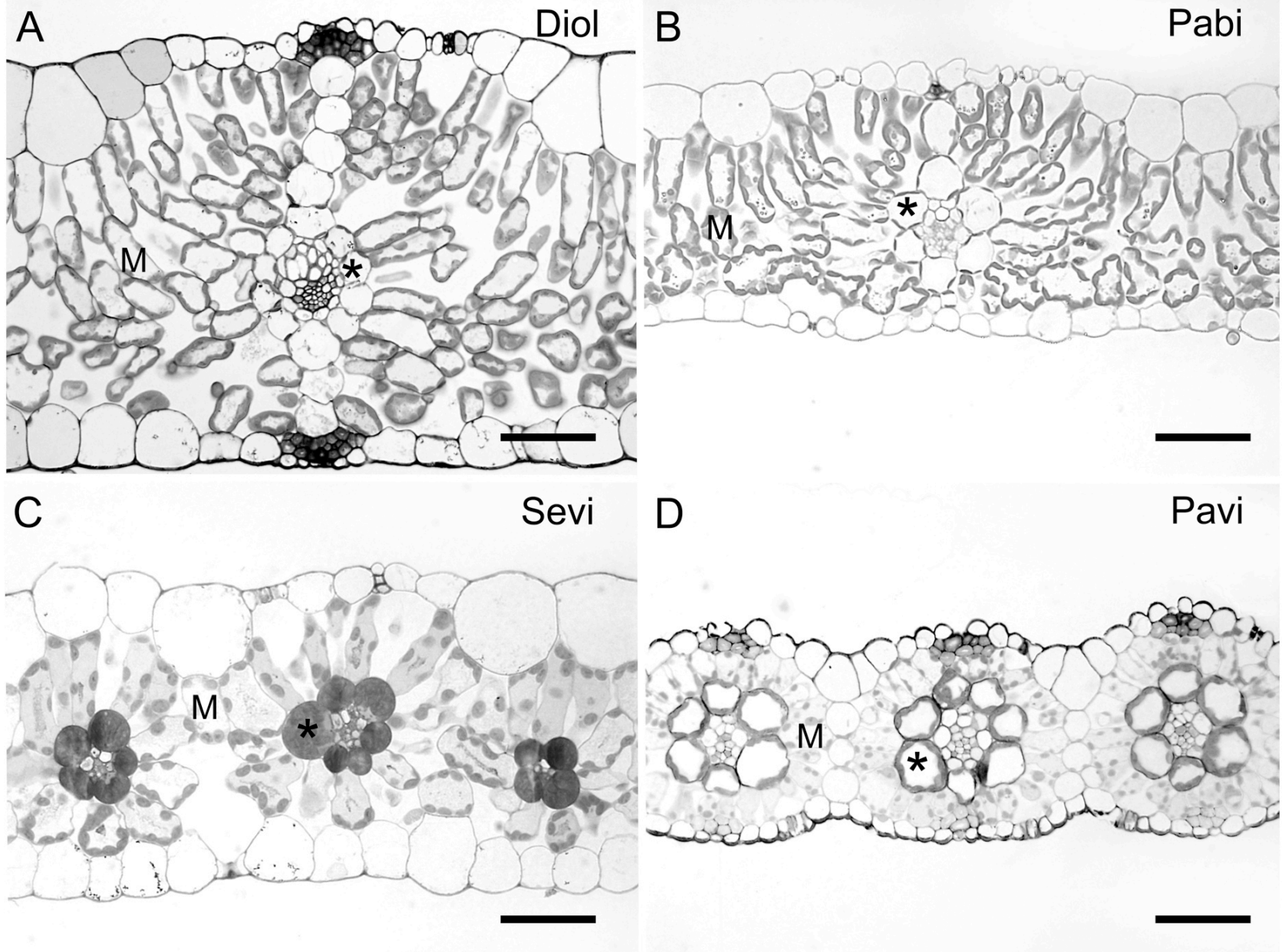
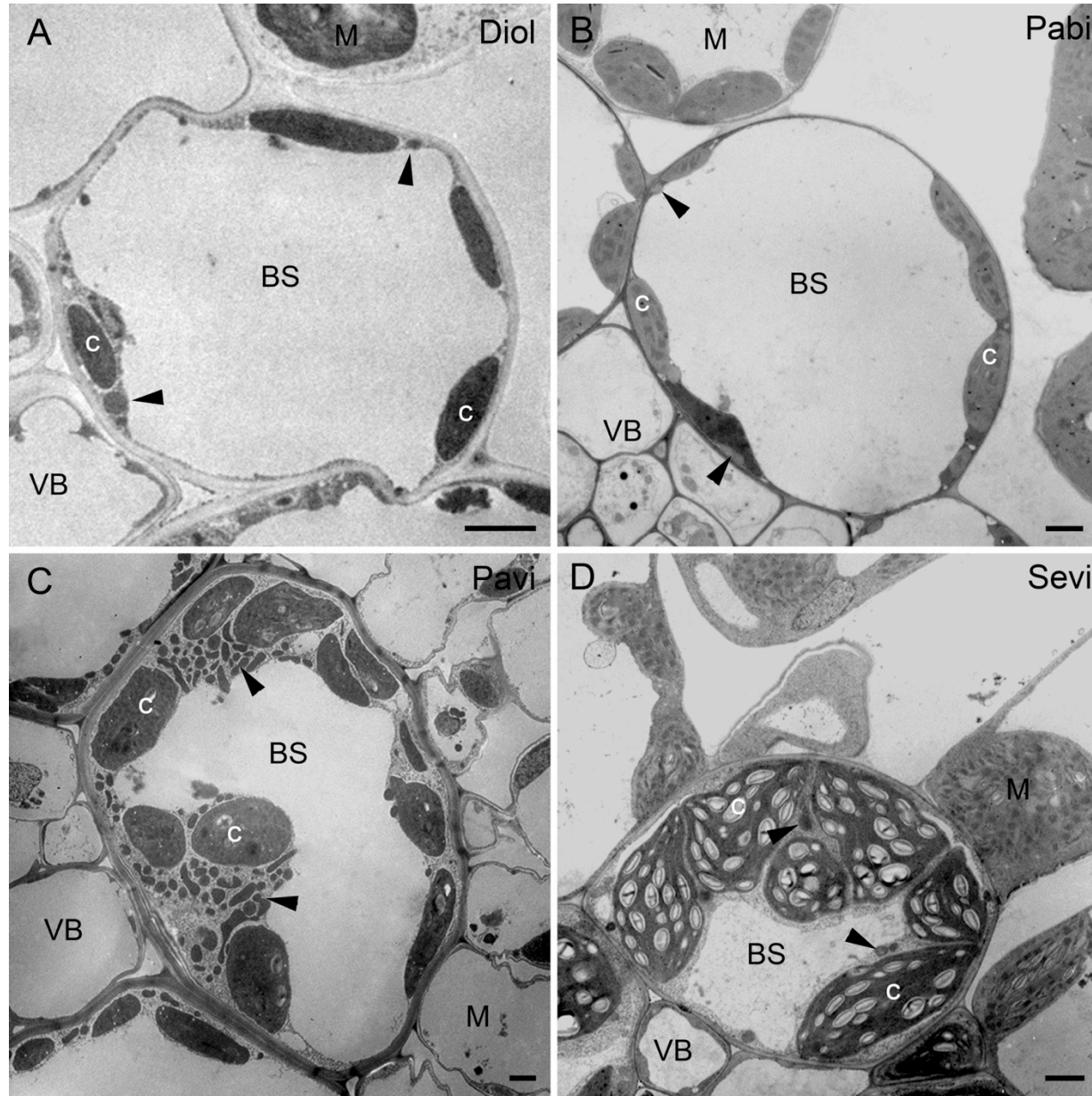


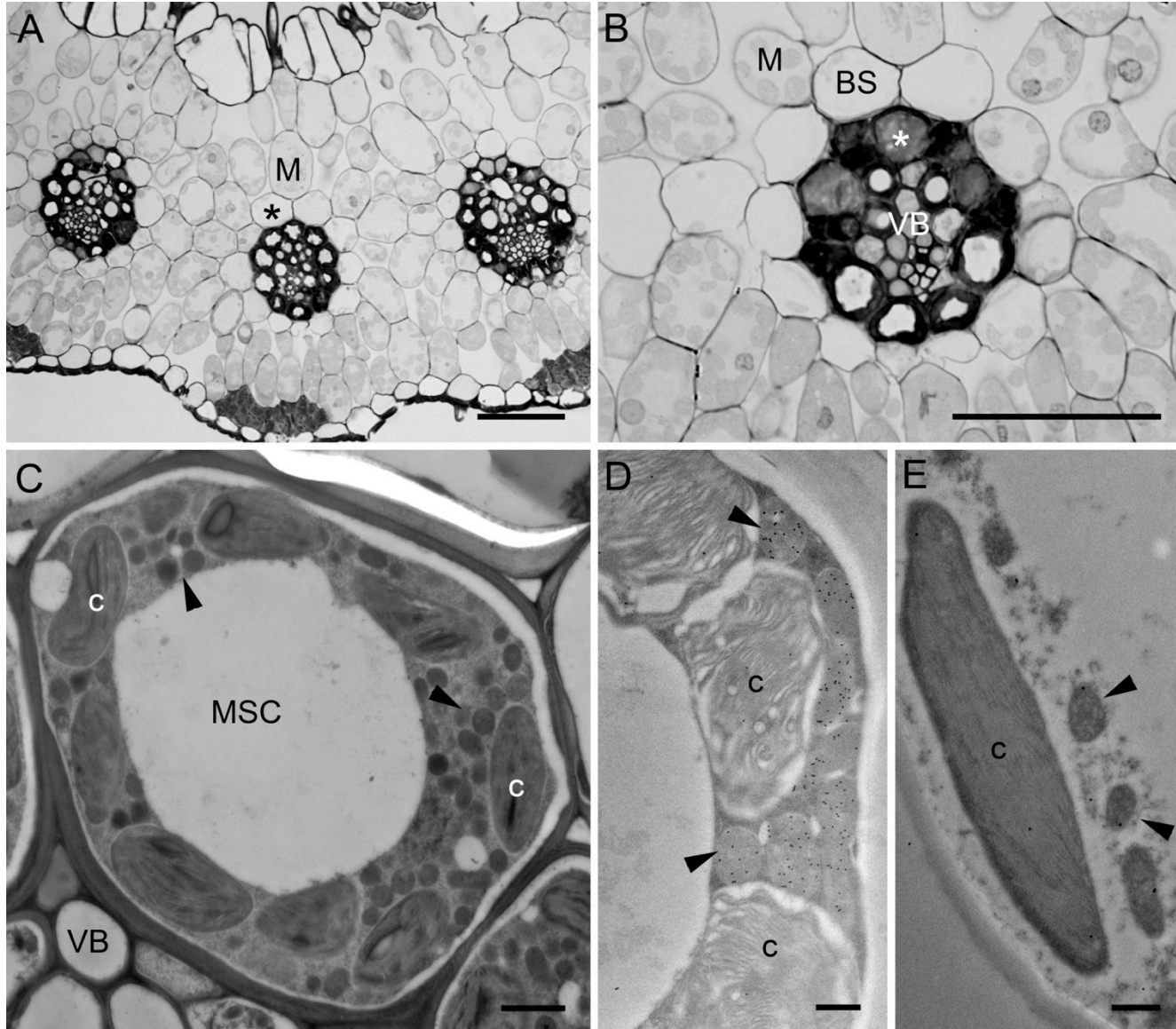
**Supplementary Figure S1.** Leaf cross sections of (A) *Dicanthelium oligosanthes* (Diol, C<sub>3</sub>); (B) *Panicum bisulcatum* (Pabi, C<sub>3</sub>); (C) *Setaria viridis* (Sevi, C<sub>4</sub>); (D) *P. virgatum* (Pavi, C<sub>4</sub>). M, mesophyll; asterisk marks bundle sheath. Bars = 50 μm.



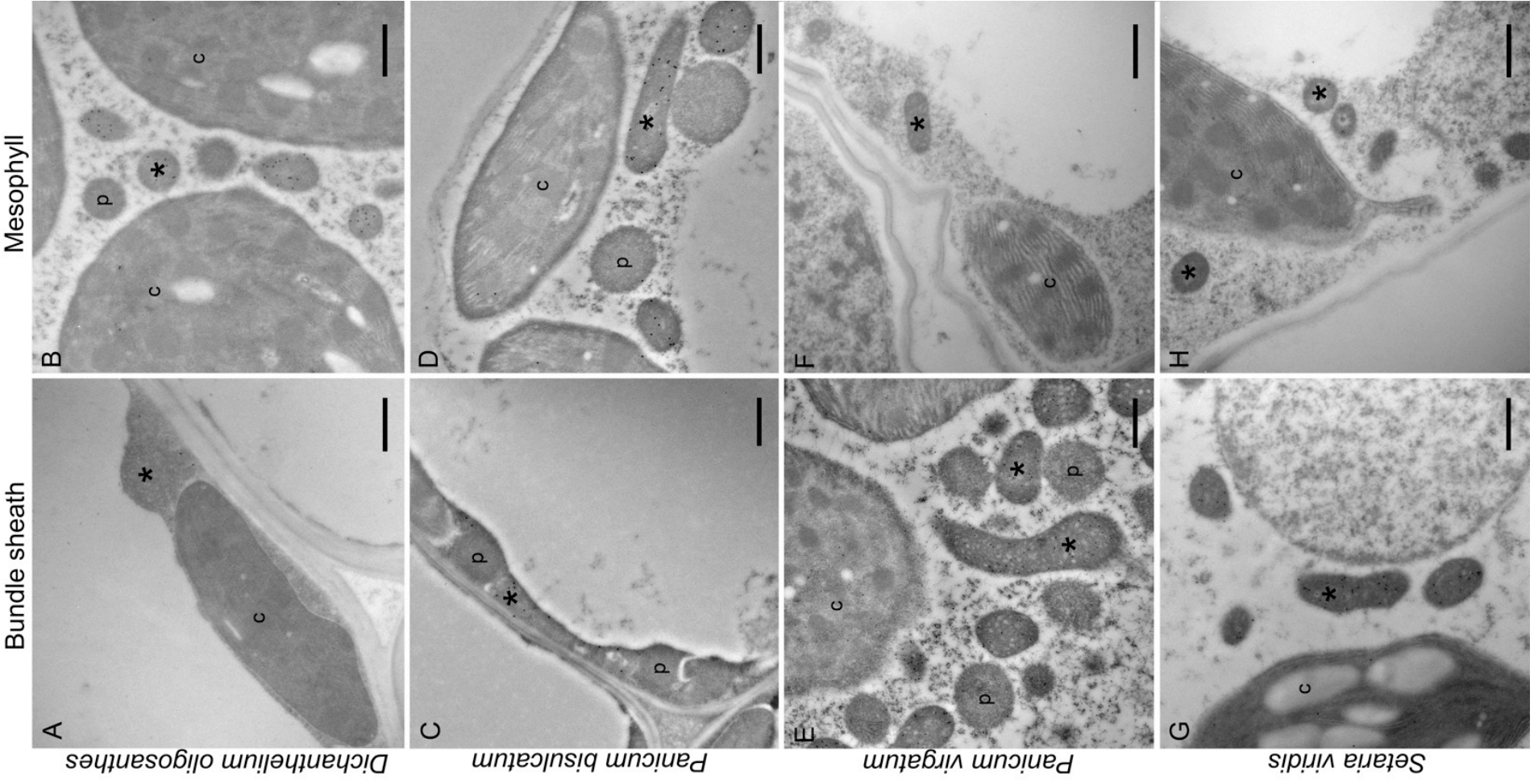
**Supplementary Figure S2.** Ultrastructure of C<sub>3</sub> and C<sub>4</sub> bundle sheath cells from (A) *Dicanthelium oligosanthos* (Diol, C<sub>3</sub>); (B) *Panicum bisulcatum* (Pabi, C<sub>3</sub>); (C) *P. virgatum* (Pavi, C<sub>4</sub>) and (D) *Setaria viridis* (Sevi, C<sub>4</sub>). BS, bundle sheath; M, mesophyll; VB, vascular tissue; c, chloroplast; arrowheads mark mitochondria. Bars = 2 μm.



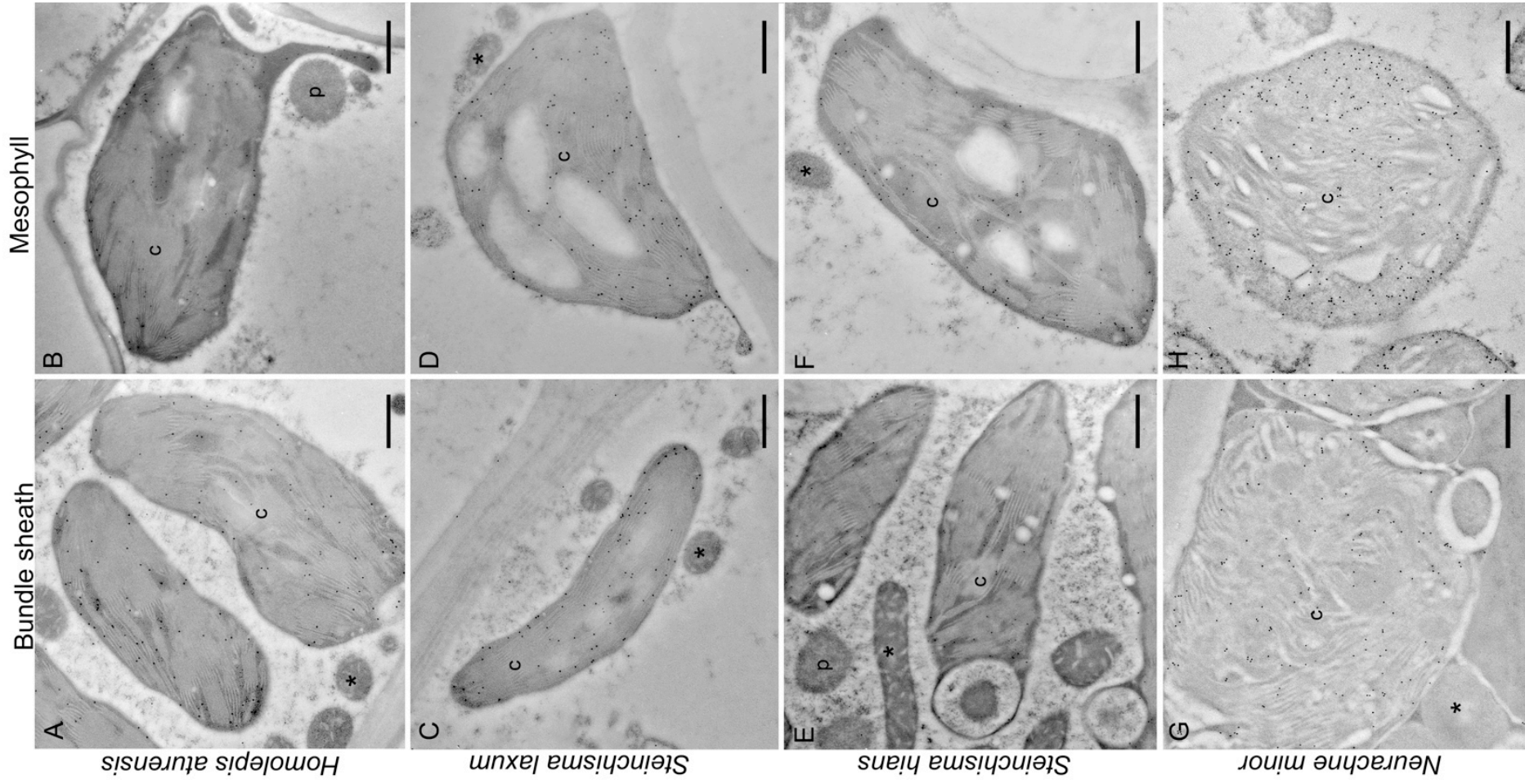
**Supplementary Figure S3.** Leaf structure and immunogold labeling of GLDP in *Neurachne minor*. (A-B) low and high magnification image of leaf illustrating mestome sheath cells (white asterisk). (C) Organelle enriched mestome sheath cell. (D-E) immunogold labeling for GLDP in mestome sheath (D) and mesophyll (E). M, mesophyll; BS, bundle sheath; VB, vascular tissue; c, chloroplast; arrowheads mark mitochondria; black asterisk marks bundle sheath. Bars = 50  $\mu\text{m}$  for A and B; 2  $\mu\text{m}$  for C; 500 nm for D and E.



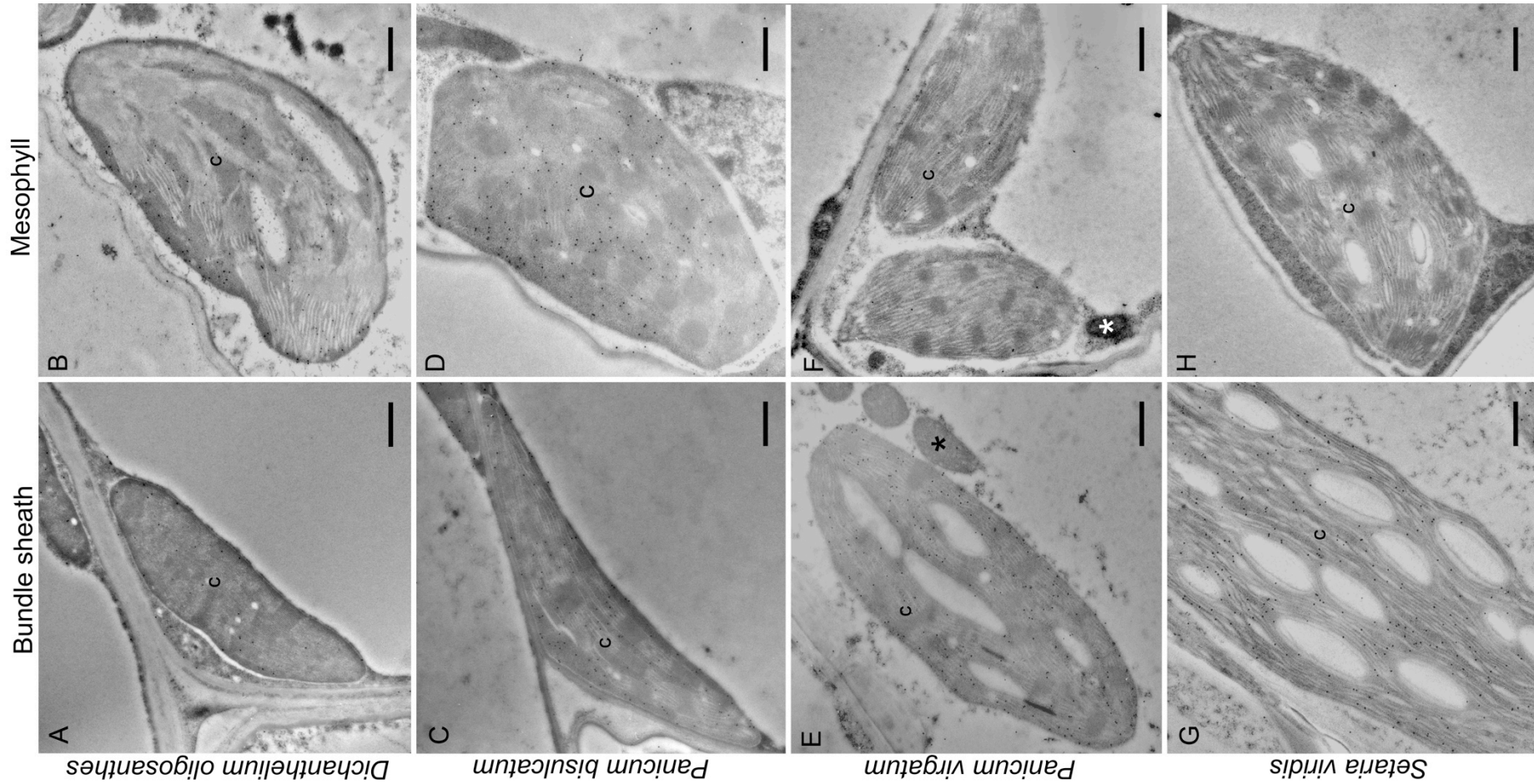
**Supplementary Figure S4.** Immunogold labeling of GLDP in the bundle sheath and mesophyll cells of (A-B) *Dichanthelium oligosanthes* ( $C_3$ ); (C-D) *Panicum bisulcatum* ( $C_3$ ), (E-F) *P. virgatum* ( $C_4$ ) and (G-H) *Setaria viridis* ( $C_4$ ). p, peroxisomes; c, chloroplasts; asterisk marks mitochondria. Bars = 500 nm.



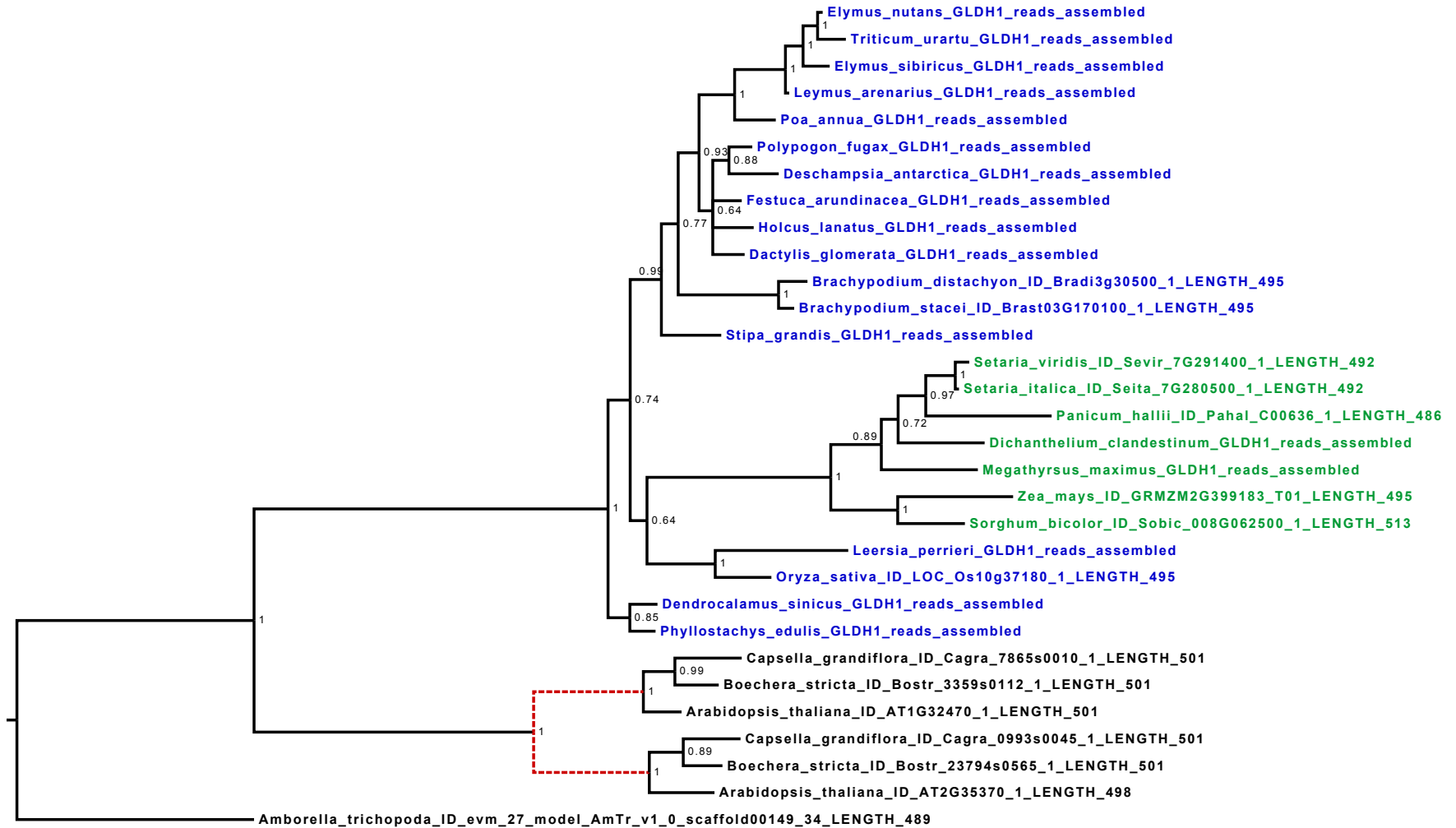
**Supplementary Figure S5.** Immunogold labeling for Rubisco large subunit in the bundle sheath and mesophyll cells of (A-B) *Homolepis aturensis*, (C-D) *Steinchisma laxum*, (E-F) *S. hians*, and (G-H) *Neurachne minor*. c, chloroplast; p, peroxisome; asterisk marks mitochondria. Bars = 500 nm.



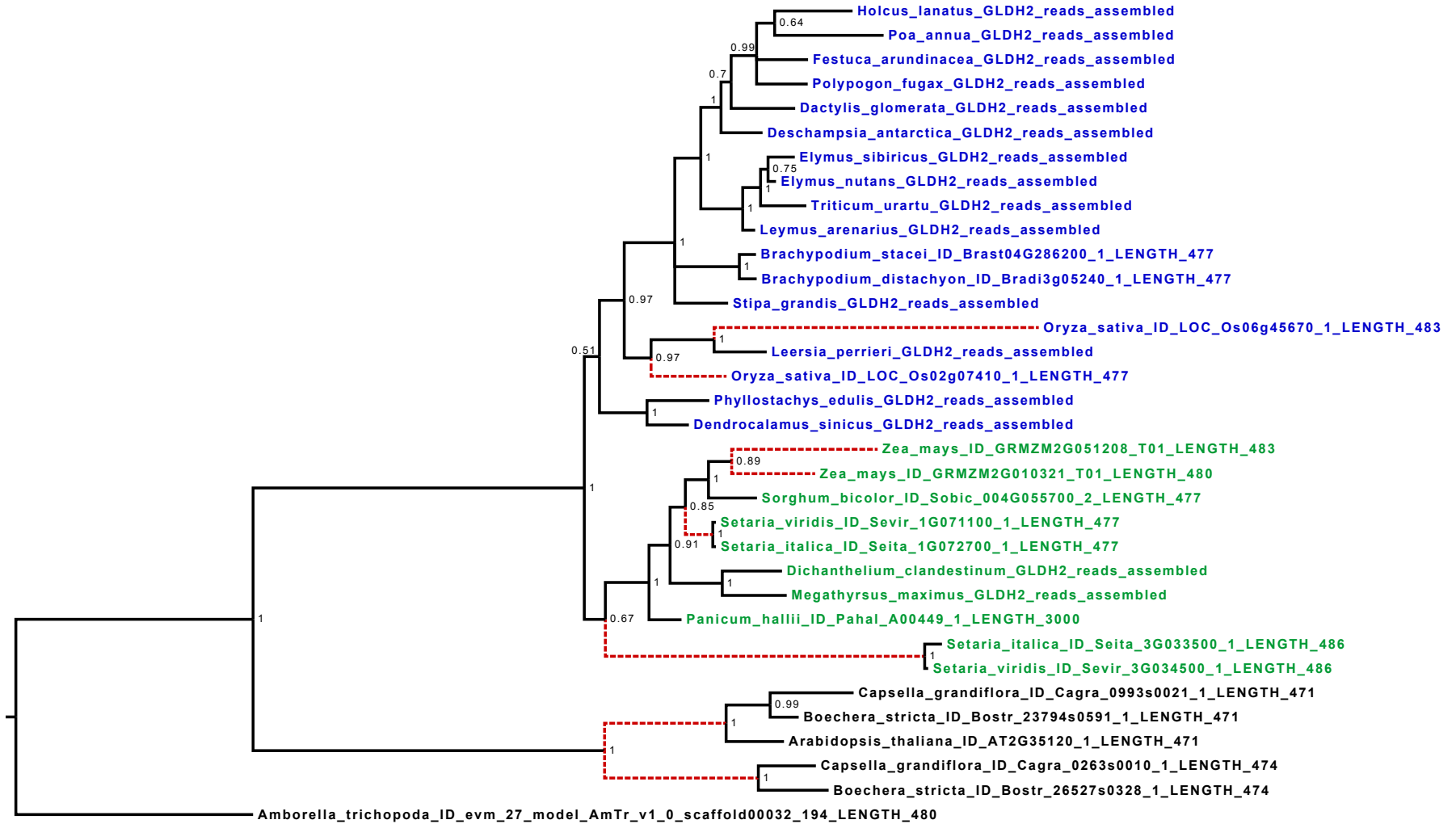
**Supplementary Figure S6.** Immunogold labeling for Rubisco large subunit in the bundle sheath and mesophyll cells of (A-B) *Dicanthelium oligosanthes* ( $C_3$ ); (C-D) *Panicum bisulcatum* ( $C_3$ ), (E-F) *P. virgatum* ( $C_4$ ) and (G-H) *Setaria viridis* ( $C_4$ ). p, peroxisomes; c, chloroplasts; asterisk marks mitochondria. Scale bars = 500 nm.



**Supplementary Figure S7.** A Bayesian phylogenetic tree of GLDH1, one of two GLDH paralogs conserved across all Angiosperms which includes the photorespiratory GLDH in *Arabidopsis* (AT2G35370). Dashed red lines denote inferred gene duplication events. Numbers at nodes indicate posterior probability.

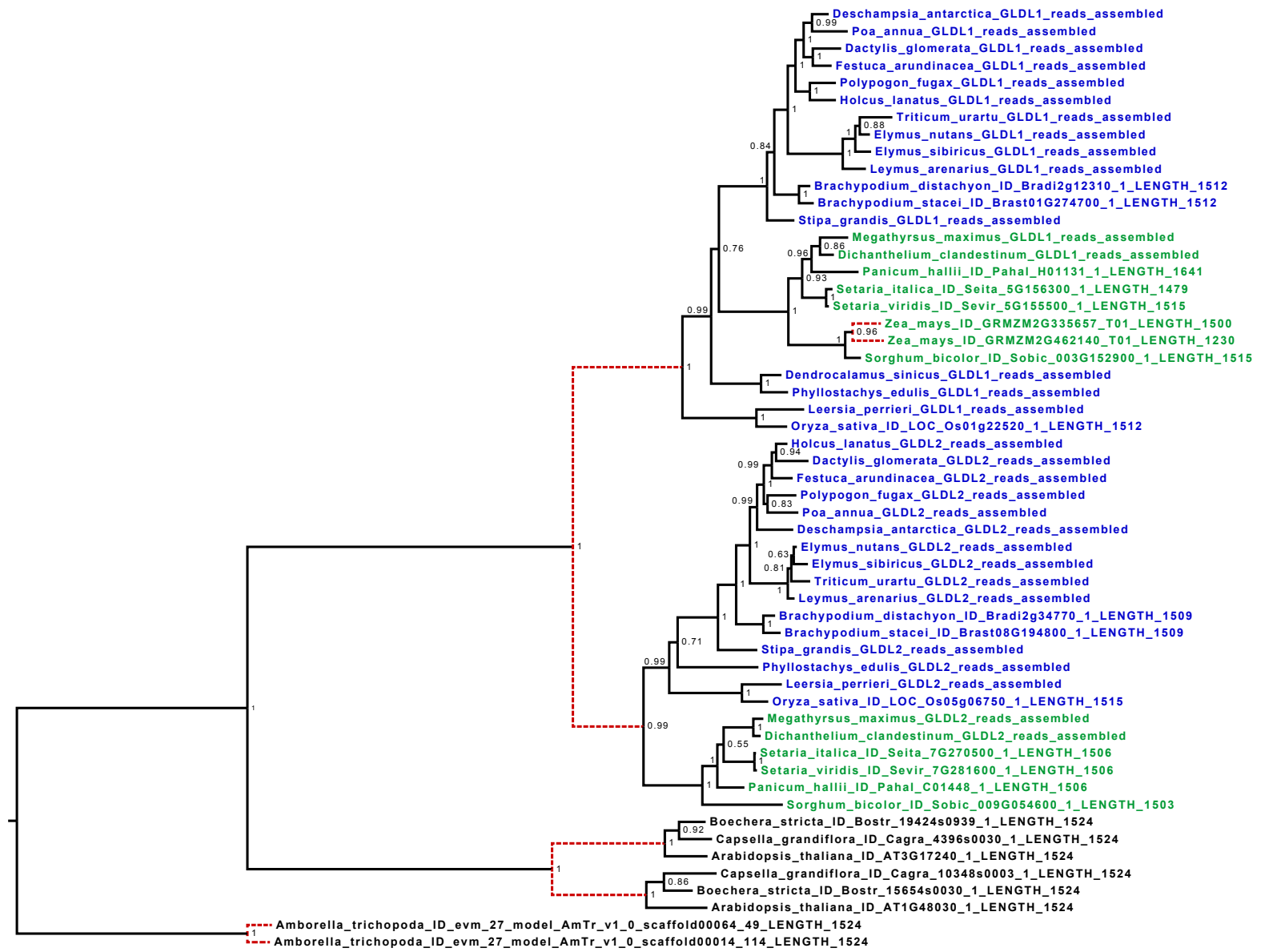


**Supplementary Figure S8.** A Bayesian phylogenetic tree of GLDH2, one of two GLDH paralogs conserved across all Angiosperms. Dashed red lines denote either gene duplication events or branches leading to duplicate copies. There is a duplication event in the Brassicaceae but *Arabidopsis* appears to have lost one copy. Numbers at nodes indicate posterior probability.





**Supplementary Figure S9.** A Bayesian phylogenetic tree of GLDL. Dashed red lines denote gene duplication events. This is the only GDC subunit with a grass-specific duplication. Most grass species examined possess both copies; however *Zea mays* and *Dendrocalamus sinicus* both appear to have lost GLDL2. Numbers at nodes indicate posterior probability.



**Supplementary Figure S10.** A Bayesian phylogenetic tree of GLDT. No duplicates were found in any of the lineages examined. Numbers at nodes indicate posterior probability.

